Progress In Electromagnetics Research, PIER 51, 27–48, 2005

SURFACE INTEGRAL EQUATION FORMULATIONS FOR LEFT-HANDED MATERIALS

D. L. Smith, L. N. Medgyesi-Mitschang, and D. W. Forester

Naval Research Laboratory, Code 5050
4555 Overlook Ave., SW, Washington D.C. 20375-5320, USA

Abstract—The electromagnetic interactions with left-handed material (LHM) medium postulated by Veselago are examined within the framework of surface integral equations (SIEs) solved by the method of moments (MM). The formulations are given for a general medium and then specialized for cases of LHM media. The scattering, propagation and lensing through such media are investigated. The implications and limitations of using SIE/MM formulations for lossless LHM media are also explored.

1. INTRODUCTION

The concept of a left-handed material (LHM)[1] was originally postulated by Veselago in the 1960's [1]. A LHM medium is one in which the real parts of both the permittivity and permeability are negative. Materials with such intrinsic properties are not known to occur in nature. However, recent experiments have shown that such properties can be simulated over limited frequencies with discrete arrangements of electrically small elements [2–4]. Proceeding from the curl form of Maxwell's equations, Veselago deduced a number of interesting properties for the behavior of time harmonic electromagnetic waves in LHM media. Recently a series of experimental and analytical investigations have examined some of the unique properties of LHM media [5–7].

In this communication we examine four cases bearing on Veselago's original conjectures using surface integral equation (SIE) formulations of Maxwell's equations solved with the Galerkin MM technique. Initially the formulations are given for a general penetrable medium with subsequent specialization to a LHM medium. Specifically we examine: (a) plane wave scattering from a conducting target surrounded by a penetrable medium, (b) radiation from a finite source embedded within a such medium, (c) propagation of a localized source outside such a medium and (d) plane wave propagation through the medium, a subcase of which is the lensing problem considered by Veselago in [1]. Finally, we discuss the implications of using SIE/MM formulations when the medium is non-causal, specifically where in a lossless LHM medium the real parts of the relative constitutive parameters, i.e., $\varepsilon'_r = \mu'_r \to -1$ as considered by Veselago.

1.1. Case a: Scattering by a p.e.c. Target Surrounded by Penetrable Medium

This problem has been studied much earlier by a number of authors. [8, 9] However, it provides a convenient starting point to lay out a hierarchy of SIE/MM formulations that encompass and test the Veselago conjectures. A generic depiction of this case is shown in Figure 1(a). The region R_1 surrounding the coated target is free space with $\varepsilon_{1r} = \mu_{1r} = 1$. A penetrable region R_2 characterized by $(\int_{2r}, B_{2r})$ and enclosed by the surface S_1 surrounds the target. The inner core is defined by a perfectly electrically conducting (p.e.c.) surface S_2 enclosing a region R_0. For generality, we assume that both $\int_{2r}$ and B_{2r}

[1] Here the term "left-handed" is not associated with the handedness of chiral materials, but with negative refraction. This terminology was originally introduced by Veselago. Alternately, LHM media are also called negative index materials (NIM).

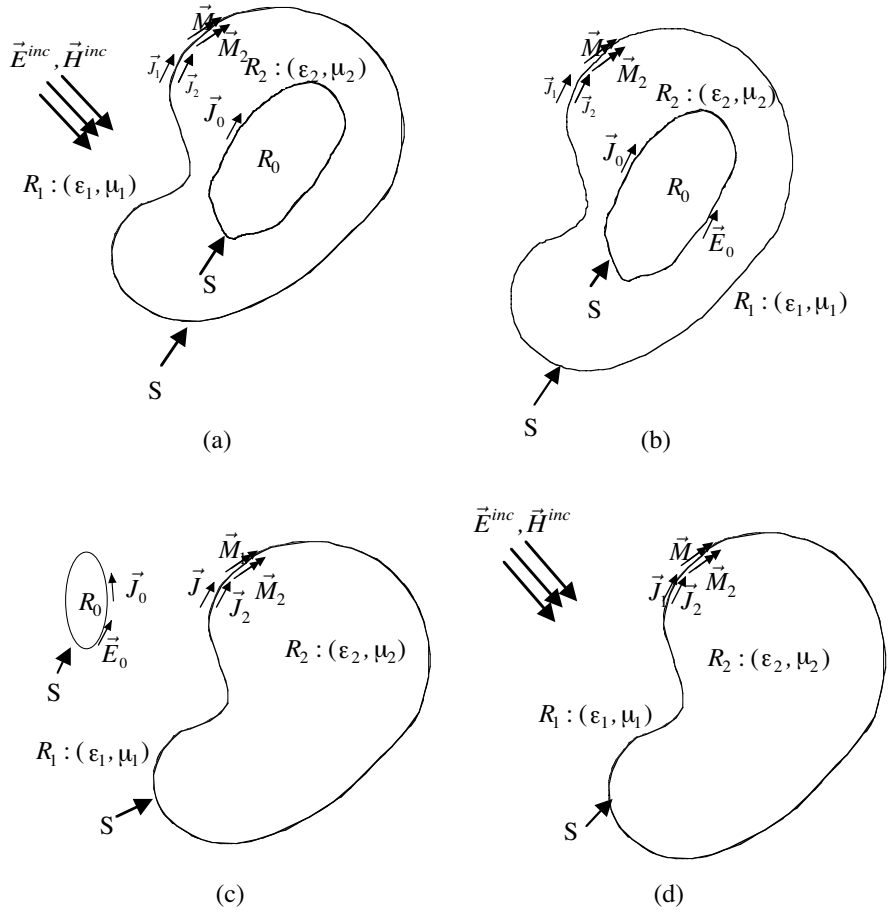

Figure 1. Generic cases– (a) plane wave illuminating a coated p.e.c. target, (b) localized source radiating from inside a penetrable region, (c) localized outside source illuminating a penetrable target, and (d) plane wave illuminating a penetrable target. The surface currents are from Schelkunoff equivalence.

may be complex having a real part that is either positive or negative. The target is illuminated by a plane wave.

Using the equivalence principle, the original problem can be replaced with equivalent electric and magnetic surface currents on surface S_1 and S_2. As shown in [8, 10] the total electric and magnetic fields in the respective regions can be written as follows. In region R_1

they are:

$$\theta(\vec{r})\vec{E}_1(\vec{r}) = \vec{E}^{inc} - L_1\vec{J}_1(\vec{r}) + K_1\vec{M}_1(\vec{r}) \quad (1)$$

$$\theta(\vec{r})\vec{H}_1(\vec{r}) = \vec{H}^{inc} - K_1\vec{J}_1(\vec{r}) - \frac{1}{\eta_1^2}L_1\vec{M}_1(\vec{r}) \quad (2)$$

Similarly for region R_2 the corresponding equations are:

$$\theta(\vec{r})\vec{E}_2(\vec{r}) = -L_2\vec{J}_2(\vec{r}) + K_2\vec{M}_2(\vec{r}) - L_2\vec{J}_0(\vec{r}) \quad (3)$$

$$\theta(\vec{r})\vec{H}_2(\vec{r}) = -K_2\vec{J}_2(\vec{r}) - \frac{1}{\eta_2^2}L_2\vec{M}_2(\vec{r}) - K_2\vec{J}_0(\vec{r}) \quad (4)$$

where $\theta(\vec{r})$ is the Heaviside function defined on the surface boundaries as

$$\theta(\vec{r}) = \begin{cases} 1, & \vec{r} \in R_i, \qquad i = 1,2 \\ \dfrac{1}{2}, & r \in \partial R_i, \quad i = 1,2 \\ 0, & \text{otherwise} \end{cases} \quad (5)$$

For notational compactness we have introduced the pair of integro-differential operators L and K above. They are defined as

$$L_i\vec{X}(\vec{r}) = \int_{\partial R_i}\left[j\omega\mu_i\vec{X}(\vec{r}\,') + \frac{j}{\omega\varepsilon_i}\nabla\nabla'\cdot\vec{X}(\vec{r}\,')\right]\Phi\left(k_i\left|\vec{r}-\vec{r}\,'\right|\right)ds' \quad (6)$$

$$K_i\vec{X}(\vec{r}) = \int_{\partial R_i}\left[\vec{X}(\vec{r}\,')\times\nabla\Phi\left(k_i\left|\vec{r}-\vec{r}\,'\right|\right)\right]ds' \quad (7)$$

where $\Phi(\cdot)$is the Green's function for an unbounded medium with the constitutive parameters $\varepsilon_i = \varepsilon_0\varepsilon_{ir}$ and $\mu_i = \mu_0\mu_{ir}$; ε_0 and μ_0 are the permittivity and permeability of free space, respectively.[2] The propagation constant $k_i = k_0\sqrt{\mu_{ir}}\sqrt{\varepsilon_{ir}}$ and k_0 is that of free space. Note the propagation constant can be that of a conventional or LHM medium.[3] The sign ambiguity of k_i associated with LHM media in the curl formulations of Maxwell's equations is avoided here. The time harmonic case with $e^{j\omega t}$ is implied. When $\vec{r} = \vec{r}\,'$ the integrals in the L and K operators are defined in the Cauchy principal value sense.

Imposing the continuity conditions on the tangential fields at surface S_1 and the vanishing of the tangential electric fields on surface

[2] For problems in 3-D, $\Phi(kR) = (4\pi R)^{-1}\exp(-jkR)$, $R = |\vec{r}-\vec{r}\,'|$; for problems in 2-D, $\Phi(kR) = j(4\pi)^{-1}H_0^{(2)}(kR)$, $R = |\vec{\rho}-\vec{\rho}\,'|$, where $H_0^{(2)}(kR)$ is the Hankel function of the zeroth order and second kind.

[3] The term "conventional medium" is one where the real parts of the permittivity $\varepsilon_r' \geq 1$ and permeability $\mu_r' \geq 1$.

S_2, yields the following coupled SIEs:

$$\left[(L_1+L_2)\vec{J}_1(\vec{r})-(K_1+K_2)\vec{M}_1(\vec{r})-L_2\vec{J}_0(\vec{r})\right]_{\tan S_1}=\vec{E}^{inc}\,|_{\tan S_1} \tag{8}$$

$$\left[(K_1+K_2)\vec{J}_1(\vec{r})+\left(\frac{1}{\eta_1^2}L_1+\frac{1}{\eta_2^2}L_2\right)\vec{M}_1(\vec{r})-K_2\vec{J}_0(\vec{r})\right]_{\tan S_1}=\vec{H}^{inc}|_{\tan S_1} \tag{9}$$

$$\left[L_2\vec{J}_1(\vec{r})-K_2\vec{M}_1(\vec{r})-L_2\vec{J}_0(\vec{r})\right]_{\tan S_2}=0 \tag{10}$$

where we have used the fact that $\vec{J}_2(\vec{r})|_{S_1} = -\vec{J}_1(\vec{r}')|_{S_1}$ and $\vec{M}_2(\vec{r})|_{S_1} = -\vec{M}_1(\vec{r}')|_{S_1}$. The surface currents $\vec{J}_0(\vec{r})$, $\vec{J}_1(\vec{r})$ and $\vec{M}_1(\vec{r})$ are the unknowns.[4]

To solve Eqs. (8)–(10), we apply the Galerkin form of the method of moments (MM) expanding the unknown surface currents in a finite set of basis functions and test the resulting system with their complex conjugates. Specifically we expand $\vec{J}_1(\vec{r})$, $\vec{M}_1(\vec{r})$ and $\vec{J}_0(\vec{r})$ as

$$\vec{J}_1(\vec{r}) = \sum_j \left\{a_{1j}\vec{f}_{1j}(\vec{r})+a_{2j}\vec{f}_{2j}(\vec{r})\right\} \tag{11}$$

$$\vec{M}_1(\vec{r}) = \eta_0\sum_j \left\{b_{1j}\vec{f}_{1j}(\vec{r})+b_{2j}\vec{f}_{2j}(\vec{r})\right\} \tag{12}$$

$$\vec{J}_0(\vec{r}) = \sum_j \left\{c_{1j}\vec{f}_{1j}(\vec{r})+c_{2j}\vec{f}_{2j}(\vec{r})\right\} \tag{13}$$

where $\eta_0 = \sqrt{\frac{\mu_0}{\varepsilon_0}}$. The coefficients a, b, and c are the corresponding unknowns in these expansions. The terms $\vec{f}_{1j}$ and $\vec{f}_{2j}$ are the elements of the basis set spanning each of the orthogonal directions on the surfaces.[5]

We form the inner products with Eqs. (8)–(10) using the complex conjugates of the basis set, i.e., $\vec{w}_{\alpha i} = (\vec{f}_{\alpha i})^*$ where $\alpha = 1, 2$. The i, j-th element of the inner products of the two operators can be written explicitly as:

$$\mathcal{L}_{ij}^{\alpha\beta}(S_1,S_2;R) = \left\langle \vec{w}_{\alpha i}(s), L\vec{f}_{\beta j}(s')\right\rangle = \iint\limits_{S_1S_2} dsds'\left\{j\omega\mu\vec{w}_{\alpha i}(s)\cdot\vec{f}_{\beta j}(s')\right.$$

[4] We have implicitly assumed that there are no internal resonances within region R_0 enclosed by S_2. If there are internal resonances, a combined formulation must be used such as given in [9, 11].

[5] For example for a 2-D problem where the object are infinite along the z-axis, the orthogonal directions are along z and t. The latter is a parametric variable describing the generating curve of the object. See [13, 14] for a full discussion of such cases.

$$+\frac{j}{\omega\varepsilon}\left(\nabla\cdot\vec{w}_{\alpha i}(s)\right)\left(\nabla'\cdot\vec{f}_{\beta j})(s')\right)\Big\}\,\Phi(k|\vec{r}-\vec{r}\,'|) \quad (14)$$

$$\mathcal{K}_{ij}^{\alpha\beta}(S_1,S_2;R) = \left\langle\vec{w}_{\alpha i}(s),\vec{f}_{\beta j}(s')\right\rangle = \eta_0\iint\limits_{S_1S_2} dsds'\vec{w}_{\alpha i}(s)$$
$$\cdot\left\{\vec{f}_{\beta j}(s')\times\nabla\Phi(k|\vec{r}-\vec{r}\,'|)\right\} \quad (15)$$

where the parameters $R, B, \int$ refer to the region where the operators are evaluated. Similar expressions can be written for $\mathcal{L}_{ij}^{\alpha\beta}(S_1,S_1;R)$, $\mathcal{L}_{ij}^{\alpha\beta}(S_2,S_2;R)$, $\mathcal{K}_{ij}^{\alpha\beta}(S_1,S_1;R)$ and $\mathcal{K}_{ij}^{\alpha\beta}(S_1,S_1;R)$. Using these Galerkin transformed operators, Eqs. (8)–(10) written in a general matrix form become:

$$\begin{bmatrix} Z_{11} & Z_{12} & Z_{13} \\ Z_{21} & Z_{22} & Z_{23} \\ Z_{31} & Z_{32} & Z_{33} \end{bmatrix}\begin{bmatrix} I_1 \\ I_2 \\ I_3 \end{bmatrix} = \begin{bmatrix} V_1 \\ V_2 \\ V_3 \end{bmatrix} \quad (16)$$

where the i,j-th element of the submatrices are:

$$(Z_{11})_{ij} = \mathcal{L}_{ij}^{\alpha\beta}(S_1,S_1;R_1)+\mathcal{L}_{ij}^{\alpha\beta}(S_1,S_1;R_2) \quad (16a)$$
$$(Z_{21})_{ij} = -(Z_{12})_{ij} = \mathcal{K}_{ij}^{\alpha\beta}(S_1,S_1;R_1)+\mathcal{K}_{ij}^{\alpha\beta}(S_1,S_1;R_2) \quad (16b)$$
$$(Z_{22})_{ij} = \frac{1}{\eta_1^2}\mathcal{L}_{ij}^{\alpha\beta}(S_1,S_1;R_1)+\frac{1}{\eta_2^2}\mathcal{L}_{ij}^{\alpha\beta}(S_1,S_1;R_2) \quad (16c)$$
$$(Z_{31})_{ij} = \mathcal{L}_{ij}^{\alpha\beta}(S_2,S_1;R_2) \quad (16d)$$
$$(Z_{13})_{ij} = -\mathcal{L}_{ij}^{\alpha\beta}(S_1,S_2;R_2) \quad (16e)$$
$$(Z_{32})_{ij} = -\mathcal{K}_{ij}^{\alpha\beta}(S_2,S_1;R_2) \quad (16f)$$
$$(Z_{23})_{ij} = -\mathcal{K}_{ij}^{\alpha\beta}(S_1,S_2;R_2) \quad (16g)$$
$$(Z_{33})_{ij} = -\mathcal{L}_{ij}^{\alpha\beta}(S_2,S_2;R_2) \quad (16h)$$

and

$$I_{1j} = a_{\beta j};\quad I_{2j} = b_{\beta j};\quad I_{3j} = c_{\beta j} \quad (16i)$$
$$V_{1i} = \mathcal{E}_i^{inc} = \left\langle\vec{w}_{\alpha i},\vec{E}^{inc}\right\rangle;\ V_{2i} = \mathcal{H}_i^{inc} = \left\langle\vec{w}_{\alpha i},\vec{H}^{inc}\right\rangle;\ V_{3i}=0 \quad (16j)$$

The submatrices in Eq. (16) represent all the electromagnetic interactions between the two surfaces S_1 and S_2. The i-th element of the RHS of Eq. (16) denotes the inner product of the testing function and the incident electric and magnetic fields on surface S_1.

The foregoing matrix equation is solved for the unknown expansion coefficients in Eqs. (11)–(13) using conventional direct or iterative methods. Knowing these coefficients, the electric and magnetic fields are uniquely determined everywhere. Detailed expressions for numerical implementation of the terms in Eq. (16) and following are given in [14].

1.2. Case b: Source inside Penetrable Region

In this case shown in Figure 1(b), the source is an electric field $\vec{E}_0$ impressed on the p.e.c. surface S_2 enclosing region R_0.[6] The total electric and magnetic fields in the respective regions in terms of the equivalent currents on the various surfaces are as follows. The fields in region R_1 are:

$$\theta(\vec{r})\vec{E}_1(\vec{r}) = -L_1\vec{J}_1(\vec{r}) + K_1\vec{M}_1(\vec{r}) \tag{17}$$

$$\theta(\vec{r})\vec{H}_1(\vec{r}) = -K_1\vec{J}_1(\vec{r}) - \frac{1}{\eta_1^2}L_1\vec{M}_1(\vec{r}) \tag{18}$$

and similarly in region R_2

$$\theta(\vec{r})\vec{E}_2(\vec{r}) = -L_2\vec{J}_2(\vec{r}) + K_2\vec{M}_2(\vec{r}) - L_2\vec{J}_0(\vec{r}) \tag{19}$$

$$\theta(\vec{r})\vec{H}_2(\vec{r}) = -K_2\vec{J}_2(\vec{r}) - \frac{1}{\eta_2^2}L_2\vec{M}_2(\vec{r}) - K_2\vec{J}_0(\vec{r}) \tag{20}$$

Imposing the boundary conditions on the exterior and interior surfaces in Figure 1(b), one obtains a system of SIEs.[7] As before application of the Galerkin procedure, yields a system matrix identical to that in Eq. (16). The RHS of Eq. (16) becomes: $V_1 = V_2 = 0$ (i.e., no incident fields) and $V_3 =< \vec{w}_{\alpha i},\ \vec{E}_0 >$, where $\vec{E}_0$ is the impressed field of the source over the surface S_2.[8]

1.3. Case c: Localized Source outside Penetrable Region

A generic depiction of this case is given in Figure 1(c). The case of a line source illuminating a homogeneous LHM slab discussed in [4], is a subcase of the present problem. Let the source consist of an electric field $\vec{E}_0$ impressed on the p.e.c. surface S_2 enclosing region R_0.

[6] This impressed field could be localized over S_2 as in the case of an aperture antenna embedded in S_2.

[7] Again it is assumed that there are no internal resonances within region R_0.

[8] In a practical problem if the source is an antenna embedded in S_2, then E_0 is the electric field over the antenna aperture.

The surrounding region R_1 is free space. The penetrable region R_2 characterized by $(\varepsilon_{2r}, B_{2r})$ is enclosed by the surface S_1. Again the fields in region R_1 are:

$$\theta(\vec{r})\vec{E}_1(\vec{r}) = -\vec{E}_0 - L_1\vec{J}_1(\vec{r}) + K_1\vec{M}_1(\vec{r}) - L_1\vec{J}_0(\vec{r}) \tag{21}$$

$$\theta(\vec{r})\vec{H}_1(\vec{r}) = -K_1\vec{J}_1(\vec{r}) - \frac{1}{\eta_1^2}L_1\vec{M}_1(\vec{r}) - K_1\vec{J}_0(\vec{r}) \tag{22}$$

and similarly in region R_2

$$\theta(\vec{r})\vec{E}_2(\vec{r}) = -L_2\vec{J}_2(\vec{r}) + K_2\vec{M}_2(\vec{r}) \tag{23}$$

$$\theta(\vec{r})\vec{H}_2(\vec{r}) = -K_2\vec{J}_2(\vec{r}) - \frac{1}{\eta_2^2}L_2\vec{M}_2(\vec{r}) \tag{24}$$

Imposing the boundary conditions on S_1 and S_2 and applying the Galerkin procedure yields a matrix equation whose elements are similar to those in Eq. (16) except now that the operators in row 3 and column 3 are evaluated in region R_1 instead of R_2, i.e.,

$$Z_{31} = \mathcal{L}_{ij}^{\alpha\beta}(S_2, S_1; R_1) \tag{25a}$$

$$Z_{13} = \mathcal{L}_{ij}^{\alpha\beta}(S_1, S_2; R_1) \tag{25b}$$

$$Z_{32} = -\mathcal{K}_{ij}^{\alpha\beta}(S_2, S_1; R_1) \tag{25c}$$

$$Z_{23} = \mathcal{K}_{ij}^{\alpha\beta}(S_1, S_2; R_1) \tag{25d}$$

$$Z_{33} = \mathcal{L}_{ij}^{\alpha\beta}(S_2, S_2; R_1) \tag{25e}$$

Since the only source is the excitation $\vec{E}_0$ on surface S_2, the RHS of Eq. (16) is $V_1 = 0;\ V_2 = 0;\ V_3 = -<\vec{w}_{\alpha i}, \vec{E}_0>$. Note here V_3 is the negative of the same term in Case b.

1.4. Case d: Plane Wave Illumination of Penetrable Region

This case is depicted in Figure 1(d). It is a generalization of the lens problems discussed by Veselago. See Fig. 5 in [1]. The surface S_1 enclosing the penetrable region R_2 (i.e., the lens) is illuminated with a plane wave. Using the equivalent current representation in Fig. 1(d) and applying the MM Galerkin procedure, yields a system matrix of the form:

$$\begin{bmatrix} Z_{11} & Z_{12} \\ Z_{21} & Z_{22} \end{bmatrix} \begin{bmatrix} I_1 \\ I_2 \end{bmatrix} = \begin{bmatrix} V_1 \\ V_2 \end{bmatrix} \tag{26}$$

where the elements of the matrix are given in Eqs. (16a)–(16c), (16i) and (16j). This matrix system is reduced to a 2×2 block since there is

only one surface S_1 on which the boundary conditions for the tangential electric and magnetic fields are imposed.

2. IMPLICATIONS OF A LHM MEDIUM

In the foregoing derivations we purposely left the permittivity and permeability of the penetrable medium unspecified so that the derivations may apply equally well for conventional and LHM media. In a conventional medium, the propagation constant is

$$\begin{aligned} k &= k_0\sqrt{\varepsilon_r\mu_r} = k_0\sqrt{\varepsilon_r' - j\varepsilon_r''}\sqrt{\mu_r' - j\mu_r''} \\ &= k_0(k_r' - jk_r'') \end{aligned} \tag{27}$$

For a LHM medium, the corresponding constant is

$$\begin{aligned} k^- &= k_0\sqrt{\varepsilon_r\mu_r} = k_0\sqrt{-\varepsilon_r' - j\varepsilon_r''}\sqrt{-\mu_r' - j\mu_r''} \\ &= j^2 k_0\sqrt{\varepsilon_r' + j\varepsilon_r''}\sqrt{\mu_r' + j\mu_r''} = -k_0(k_r' + jk_r'') \\ &= -k^* \end{aligned} \tag{28}$$

where k^* is the complex conjugate of the (complex) propagation constant of the corresponding conventional medium. Noting that the $\Phi(k^- R) = \Phi(-k^* R)$, $\nabla\Phi(k_2^- R) = -\nabla\Phi(k_2^* R)$ and $\eta_-^2 = (\eta^2)^*$, it can be shown that the Galerkin transformed operators in the LHM medium are the negative of the complex conjugate of the operators for a conventional medium, i.e., $\mathcal{L}^- = -\mathcal{L}^*$ and $\mathcal{K}^- = -\mathcal{K}^*$. Using the relationships in Eqs. (14)–(15) yields

$$\mathcal{L}_{ij}^{\alpha\beta-}(S_1, S_2; R) = -\left(\mathcal{L}_{ij}^{\alpha\beta}(S_1, S_2; R)\right)^* \tag{29}$$

$$\mathcal{K}_{ij}^{\alpha\beta-}(S_1, S_2; R) = -\left(\mathcal{K}_{ij}^{\alpha\beta}(S_1, S_2; R)\right)^* \tag{30}$$

Thus the matrix elements for the LHM medium can be formed from the corresponding ones for a conventional medium.

3. A LIMITING CASE

A special situation arises for a lossless LHM medium as the real parts of the relative permittivity $\varepsilon_{1r}' \to -1$ and permeability $\mu_{1r}' \to -1$. For brevity we designate this limiting case here as "negative" free space (NFS). It was used by Veselago to articulate several properties of LHM media. [1] In the NFS case, several of the submatrix blocks

in the system matrices of the SIE/MM formulations, associated with Cases (a)–(d) discussed above, become null matrices. For example, the submatrix blocks in Eq. (16), i.e., Z_{11}, Z_{12}, Z_{21} and Z_{22} are null matrices making the system insoluble. It may seem strange that a SIE/MM formulation that is well-posed for a conventional medium, is not well-posed for a NFS one until one realizes that the latter medium is non-physical since it violates causality.[9] The null matrices in the SIE/MM formulations are mathematical reflections of this fact. For a LHM medium where $\varepsilon'_{2r} = \mu'_{2r} = -1$ and lossy ($\varepsilon''_r \neq 0,\ \mu''_r \neq 0$), or $\varepsilon'_{2r} \neq -1$ and $\mu'_{2r} \neq -1$ and lossless, the foregoing formulations yield well behaved results as illustrated below.[10]

4. DISCUSSION OF EXAMPLES

Representative numerical calculations were carried out for several of the foregoing cases using the MM-based CARLOS software. [15, 16] Convergent results were achieved throughout with a 10/8 surface discretization. As an example of Case (b), Fig. 2 depicts the results for a source embedded in a penetrable region. For this case the penetrable region is an infinite (2-D) slab with a cross sectional area of $10.16\,\lambda \times 3.387\,\lambda$. The cylindrical (line) source is located at the center of the slab, polarized perpendicular to the cross sectional area of the slab. The frequency of the source is 10 GHz. The results for a lossy LHM medium with $\varepsilon_r = -2.0 - j0.2$ and $\mu_r = -1.0 - j0$, are contrasted with that for a conventional medium with $\varepsilon_r = 2.0 - j0.2$ and $\mu_r = 1.0 - j0$. Examining the map of the ultra-near electric field intensities for the LHM slab, we observe a field concentration ("focusing") on either side of the slab, absent in the conventional medium slab. This effect has also been observed previously in FDTD calculations. [4] At 10 GHz the slab is $3.387\,\lambda$ thick. In passing it should be noted that via a ray trace argument, one can show that this field concentration is due to negative refraction effects inherent in a LHM medium as postulated by Veselago. However, ray tracing only accounts for one of the electromagnetic effects present here, namely refraction. Since the slab has finite height

[9] The Kramers-Kronig relationships require that there be loss when the permittivity or permeability becomes negative. Note in FDTD calculations of the EM fields are postulated on the causal behavior of a material constituting the penetrable region. In time harmonic analysis, this is not *a priori* requirement. However as our discussion shows, the lack of causality leads to a mathematically ill-posed problem for NFS.

[10] For nongyrotropic plasmas with $\mu_r = 1$ and ε_r can be positive or negative and also complex. For the case of a Lorentzian plasma where $\varepsilon'_r = 1 - \omega_p^2(\omega^2 + v^2)^{-1}$ and $\varepsilon''_r = \omega_p^2 v(\omega^2 + v^2)^{-1}$, if the plasma radian frequency $\omega_p \gg \omega \geq v$, then $\varepsilon'_r < -1$. SIE/MM formulations have been successful in modeling these cases. In the lossless plasma case, the collision frequency $\Lambda = 0$. A negative permittivity requires that $\omega_p > \omega$. However, this is hard to achieve in a collisionless environment.

($10.16\,\lambda$), diffraction effects are also important. These contribute to the irregular intensity contours arising in both media in seen in Fig. 2.

Next we consider the situation of a localized source outside a penetrable region, exemplifying Case (c). First for comparison, Fig. 3 depicts the case of a cylindrical source outside an infinite "free space" slab (i.e., with $\varepsilon_r = \mu_r = 1.0$). The source is $1.524\,\lambda$ from the left side of the slab, polarized again perpendicular to the cross sectional area of the slab. The dimensions and geometry of the slab are identical with those in Fig. 2. The frequency of the source is 10 GHz. As expected the ultra-near electric fields radiated by the source are unaffected by the presence of the "free space" slab. These results were compared with calculations made in the absence of a slab. The two calculations were indistinguishable. They provide a check of the numerical algorithms used in the CARLOS code and are a reference for the results obtained for a LHM slab considered next.

Figure 4 shows the map of the ultra-near electric fields in the presence of LHM slab. The intensity and the constant phase loci are plotted. The parameters of the problem are the same as those in Fig. 3, except the permittivity and permeability of the slab are $\varepsilon_r = -3.0 - j0.0$ and $\mu_r = -1.0 - j0.0$, respectively. Note in this case the LHM medium is lossless. As seen previously for the case of the line source within a LHM slab in Fig. 2(a), a series of field concentration points exist and there is a "channeling" or "beaming" of the fields along a centerline of slab occurs. Similar trends were observed by Ziolkowski and Heyman. [5] The other prominent features are the series of "vee" shaped intensity lines within the slab, indicative of the negative refraction predicted by Veselago. The negative refraction can also be deduced from the constant phase plots. If the LHM slab is lossy, these intensity lines are much diminished. FDTD simulations have shown similar effects. There also appear to be significant surface waves on the left hand surface of the slab.

The ultra-near electric fields (intensity and phase) produced by a line source outside the slab when the permittivity $\varepsilon_r = -1.001 - j0.013$ and permeability $\mu_r = -1.001 - j0.013$ *approach* negative free space (NFS), illustrated in Fig. 5. As was discussed earlier, to use SIE/MM formulations it is necessary to have a lossy medium when $\varepsilon_r' \to -1$ and $\mu_r' \to -1$. The other parameters for this problem are unchanged from those in Fig. 4. Two mechanisms are operative here: channeled wave propagation through the slab and the presence of surface waves on the left hand boundary of the slab. This correlates well with earlier results obtained with the FDTD technique for a line source illuminated slab. [4] Additional calculations not shown here for very weakly lossy LHM media, show similar effects with the field intensities more and more

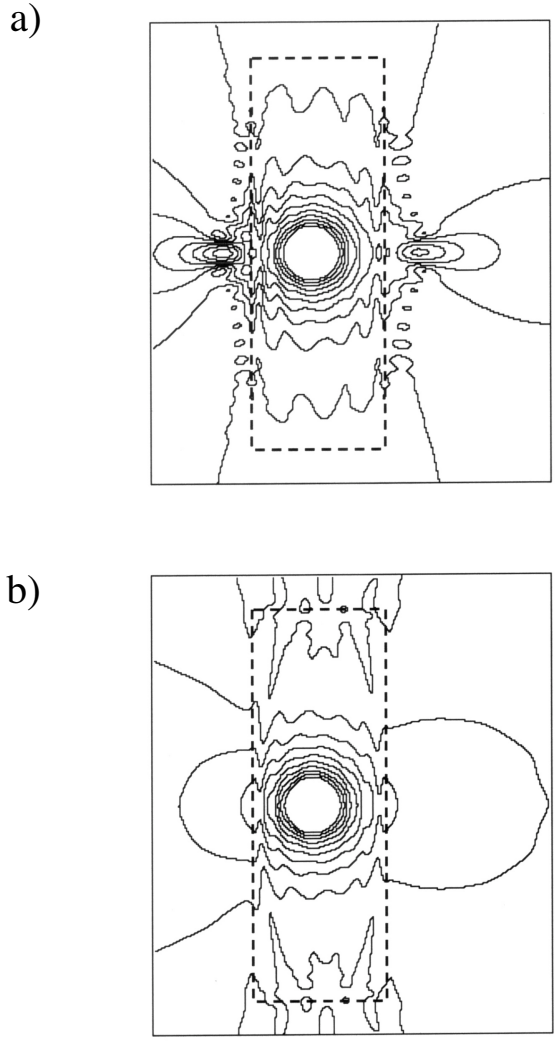

Figure 2. Contour map of the ultra-near electric field intensities due to a cylindrical (line) source embedded in an infinite penetrable slab. The cross sectional area of the slab is 12 in. $\times$ 4 in. ($10.16\,\lambda \times 3.387\,\lambda$ at 10 GHz.) The source is in the center of the slab, polarized perpendicular to the cross section of the slab. (a) lossy LHM medium with $\varepsilon_r = -2.0 - j0.2$; $\mu_r = -1.0 - j0$. (b) conventional lossy medium with $\varepsilon_r = 2.0 - j0.2$; $\mu_r = 1.0 - j0$. The intensity map is limited for visual clarity.

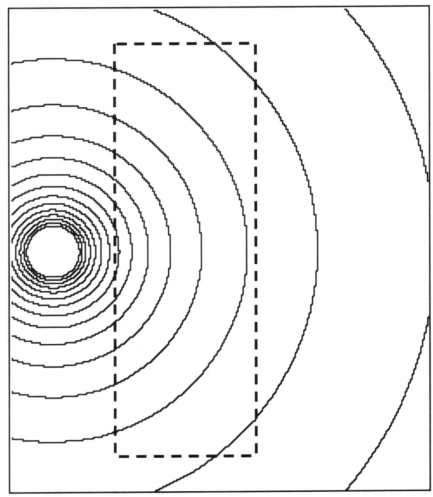

Figure 3. Contour map of the ultra-near electric field intensities due to a cylindrical (line) source outside an infinite "free space" slab with $\varepsilon_r = \mu_r = 1.0$. The source is 1.8 in. ($1.54\,\lambda$ at 10 GHz) from the left surface of the slab. It is polarized perpendicular to the cross section of the slab. The geometry of the slab is as in Fig. 2.

defocused and with the presence of secondary field intensity structures.

Finally, we explored Veselago's conjecture that convex and concave lenses "have changed places" when they are made of a LHM medium. Specifically according to this conjecture, a concave LHM lens produces converging rays resulting in focusing in the manner of a convex lens made of a conventional medium. In arriving at this result, Veselago used ray trace arguments assuming that a plane wave (parallel rays) impinged on the lens. Initially we used the formulation in Case (d) for this problem. For the numerical simulations the concave LHM lens with $\varepsilon_r = \mu_r = -2.0 - j0.0$ was finite in height (i.e., $10.1612\,\lambda$ at 10 GHz). The lens dimensions are given in Fig. 6. A plane wave illumination of this lens (and larger ones not shown here) produced significant edge diffraction masking the basic focusing effect of interest here.

As an alternative, we used fields produced by a uniform current sheet to illuminate the lens. The current sheet was $3.387\,\lambda$ wide and centered $5.08\,\lambda$ from the left hand surface of the lens at 10 GHz.[11]

[11] This arrangement can be thought of as the dual of a plane wave through a slit. The resulting field is approximately planar in the central portion of the lens. The lens problem with the finite source is an example of Case c, considered earlier.

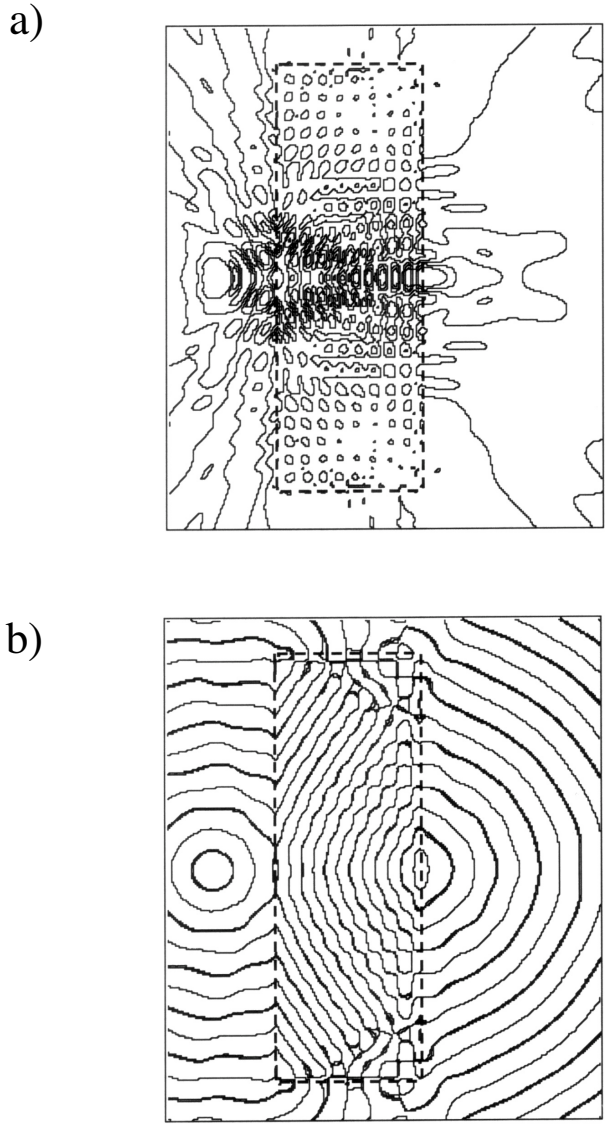

Figure 4. Contour map of the ultra-near electric fields due to a cylindrical (line) source outside an infinite lossless LHM slab with $\varepsilon_r = -3.0 - j0.0$, $\mu_r = -1.0 - j0.0$. The other parameters of the problem are as in Fig. 3. (a) amplitudes, (b) constant phase contours.

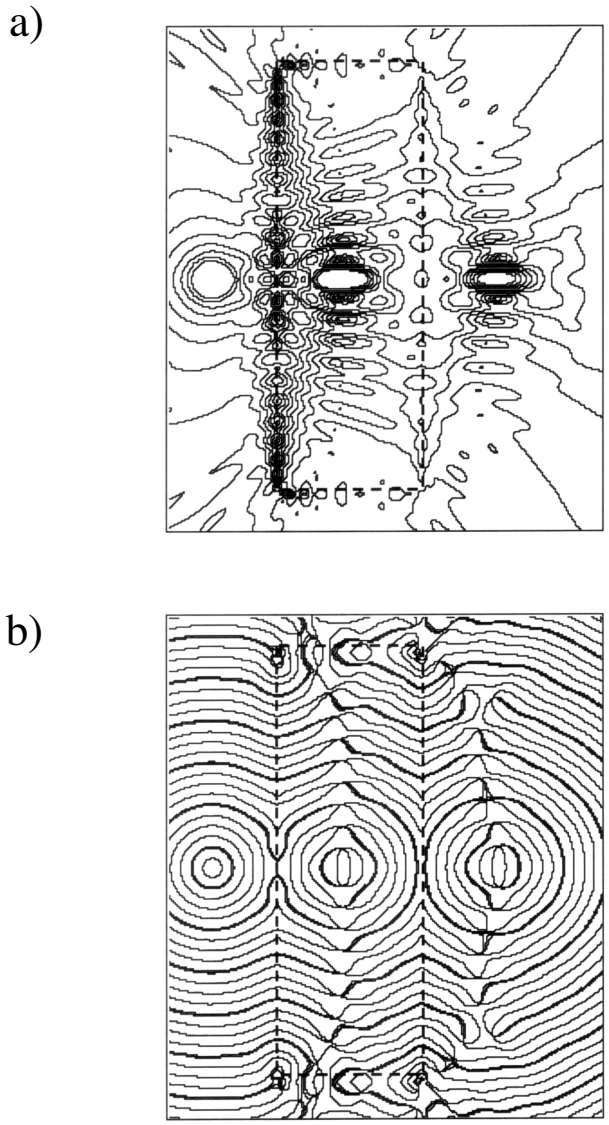

Figure 5. Contour map of the ultra-near electric fields due to a cylindrical (line) source outside an infinite lossy LHM slab with $\varepsilon_r = -1.001 - j0.013,\ \mu_r = -1.001 - j0.013$. The other parameters of the problem are as in Fig. 3. (a) amplitudes, (b) constant phase contours.

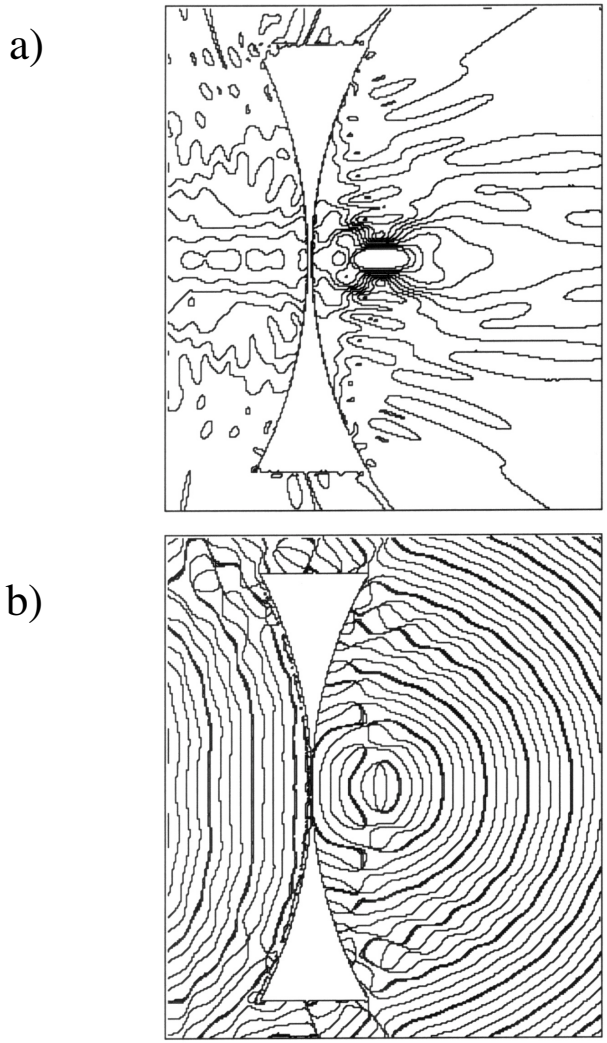

Figure 6. Contour map of the ultra-near electric fields due to a uniform sheet current source propagated through a concave 2-D lossless LHM lens with $\varepsilon_r = \mu_r = -2$. The right and left hand lens surfaces are formed by radii of curvature of $10.158\,\lambda$ and $10.97\,\lambda$, respectively. The current sheet is 4 in. ($3.387\,\lambda$) wide, centered 6 in. ($5.08\,\lambda$) from the left hand surface of the lens. The polarization is perpendicular to the cross sectional area of the lens. The frequency of the source is 10 GHz. (a) amplitudes, (b) constant phase contours.

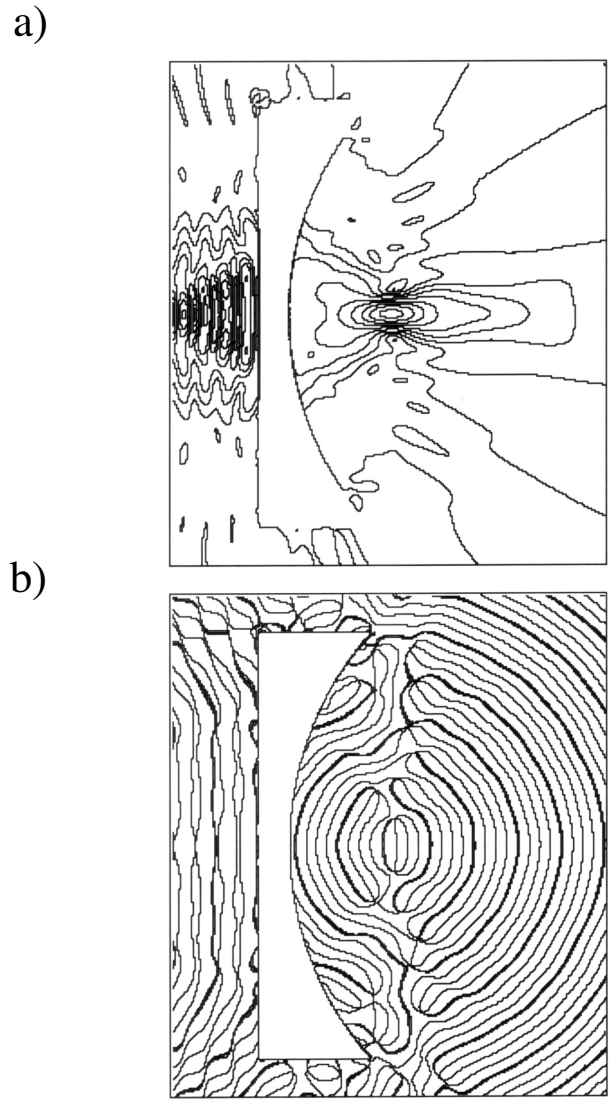

Figure 7. Contour map of the ultra-near electric fields due to an uniform sheet current source propagated through a modified concave 2-D lossless LHM lens with $\varepsilon_r = \mu_r = -2$. The source, polarization, and height and right hand curvature of the lens are those given in Fig. 6. (a) amplitudes, (b) constant phase contours.

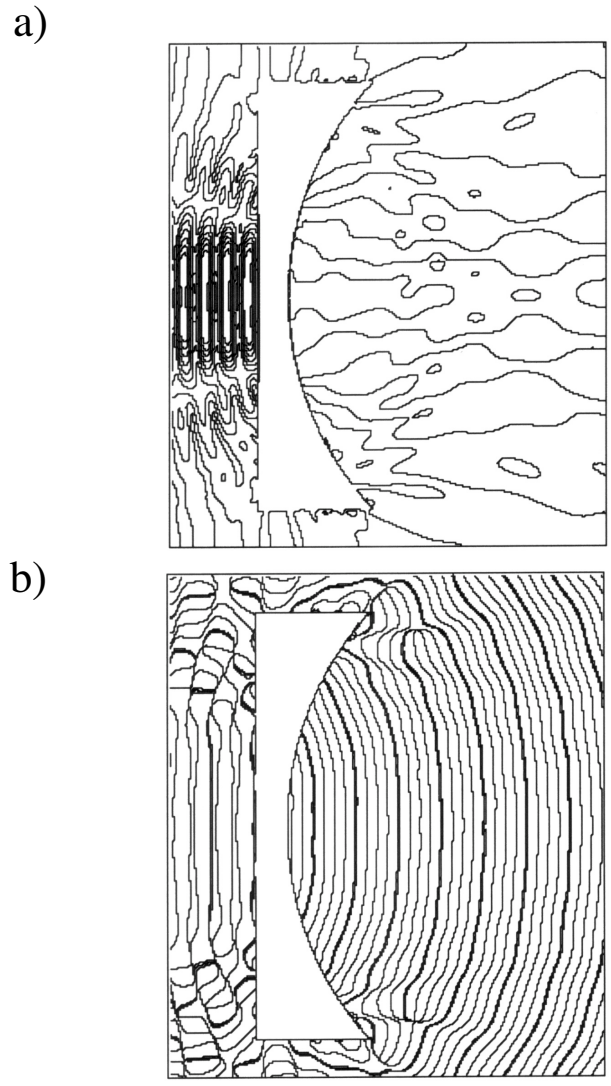

Figure 8. Contour map of the ultra-near electric fields due to an uniform sheet current source propagated through a modified concave 2-D lens with $\varepsilon_r = 2$ and $\mu_r = 1.0$. The source, polarization, and height and right hand curvature of the lens are those given in Fig. 6. (a) amplitudes, (b) constant phase contours.

The resulting electric field wave fronts were approximately planar in the central part of the lens. The field was polarized perpendicular to the cross section of the lens. Figure 6 depicts the resulting ultra-near electric fields propagated through the lens with this source. In concordance with Veselago's conjecture, the fields become focused. The irregularity of the intensity contours is principally due to edge diffraction arising from the finiteness of the lens. Parenthetically, the corresponding results for a convex lens made of a conventional medium, showed divergent fields, i.e., no focusing.

Additional numerical simulations were carried out for modified convex lenses of LHM and conventional media. A representative example for the LHM case is shown in Fig. 7. The height and right hand curvature of the lens and as well as the illuminating source are the same as those in Fig. 6. The LHM medium is $\varepsilon_r = 2.0 - j0.0$. The corresponding results for a conventional medium lens with $\varepsilon_r = 2.0 - j0.0$ and $\mu_r = 1.0 - j0.0$ are given in Fig. 8. Note in the latter case no focusing occurs. These, and other results not shown here, support the conjectures of Veselago regarding the behavior of LHM media in lenses. While his conclusions were based solely on ray trace arguments, the present results also incorporate all nonspecular electromagnetic interactions including waves and diffraction.

5. SUMMARY

We have examined four cases using SIE/MM formulations involving LHM media bearing on Veselago's original conjectures regarding the behavior of electromagnetic propagation and scattering in the presence of such media. For illustration, numerical simulations were carried out for line and distributed sources inside and outside such media. Specifically, the case of a finite planar LHM slab, and convex and modified convex LHM lenses were considered confirming Veselago's conjectures. The results were also contrasted with those for conventional media. It was shown that SIE/MM formulations are well-posed and computationally robust, except in cases where the relative permittivity and permeability are $\varepsilon_r = \mu_r = -1.0 - j0$, i.e., the "negative" free space case originally considered by Veselago.

ACKNOWLEDGMENT

This research was sponsored in part by the DARPA Metamaterials Program and the Naval Research Laboratory.

REFERENCES

1. Veselago, V. G., "The electrodynamics of substances with simultaneously negative values of $\int$ and B," *Sov. Phys. Usp.*, Vol. 10, 509, 1968.
2. Smith, D. R., W. J. Padilla, D. C. Vier, S. C. Nemat-Nasser, and S. Schultz, "A composite medium with simultaneously negative permeability and permittivity," *Phys. Rev. Lett.*, Vol. 84, 4184, 2000.
3. Rachford, F. J., D. L. Smith, P. F. Loschialpo, and D. W. Forester, "Calculations and measurements of wire and/or split-ring negative index media," *Phys. Rev. E*, Vol. 66, 036613, 2002.
4. Loschialpo, P. F., D. L. Smith, F. J. Rachford, D. W. Forester, and J. Schelleng, "Electromagnetic waves focused by a negative-index planar lens," *Phys. Rev. E*, Vol. 67, 026502 (R), 2003.
5. Ziolkowski, R. W. and E. Heyman, "Wave propagation in media having negative permittivity and permeability," *Phys. Rev. E*, Vol. 64, 056625-1, 2001.
6. Schelleng, J., C. Monzon, P. F. Loschialpo, D. W. Forester, and L. N. Medgyesi-Mitschang, "Characteristic of waves guided by a grounded 'left handed' material slab of finite extent," submitted to *Phys. Rev. E.*
7. Loschialpo, P. F., D. W. Forester, D. L. Smith, F. J. Rachford, C. Monzon, and J. Schelleng, "Optical properties of an ideal homogeneous, causal 'left handed' material slab," submitted to *Phys. Rev. E.*
8. Miller, E. K., L. N. Medgyesi-Mitschang, and E. H. Newman (Eds.), *Computational Electromagnetics: Frequency-Domain Method of Moments*, Part 4, IEEE Press, Inc. New York, 1991.
9. Huddleston, P. L., L. N. Medgyesi-Mitschang, and P. M. Putnam, "Combined field integral equation formulation for scattering by dielectrically coated conducting bodies," *IEEE Trans. Antennas Propagat.*, Vol. AP-34, 510–520, 1986.
10. Medgyesi-Mitschang, L. N., P. G. Moore, D. L. Smith, and S. G. Lambrakos, "Ultra-near fields of penetrable bodies of translation: ω-κ representations," *J. of Electromagn. Waves and Appl.*, Vol. 12, 1467–1483, 2002.
11. Mautz, J. R. and R. F. Harrington, "A combined-source solution for radiation and scattering from a perfectly conducting body," *IEEE Trans. Antennas Propagat.*, Vol. AP-27, 445–454, 1978.
12. Wallenberg, R. F. and R. F. Harrington, "Radiation from apertures in conducting cylinders of arbitrary cross section," *IEEE*

Trans. Antenna Propagat., Vol. AP-17, 56–62, 1969.

13. Medgyesi-Mitschang, L. N. and J. M. Putnam, "Scattering from finite bodies of translation: plates, curved surfaces and noncircular cylinders," *IEEE Trans.*, Vol. AP-31, 847–852, 1983.
14. Medgyesi-Mitschang, L. N., J. M. Putnam, and M. B. Gedera, "Generalized method of moments for 3-D penetrable scatterers," *J. Opt. Soc. Am. A*, Vol. 11, 1383–1398, 1994.
15. Putnam, J. M., L. N. Medgyesi-Mitschang, and M. B. Gedera, *CARLOS-3D: Three-Dimensional Method of Moments Code*, Vols. I and II, McDonnell Douglas Rpt. 10, Dec. 1992.
16. Putnam, J. M. and M. B. Gedera, "CARLOS-3D: A general purpose 3-D method of moments scattering code," *IEEE Antennas Propag. Mag.*, Vol. 35 , 69–71, 1993.

D. L. Smith received his Ph.D. in physics from the University of Illinois in 1989. He pursued postdoctoral studies at the Microwave Technologies Division of the Naval Research Laboratory (NRL) investigating the development of electronic devices with large band-gap materials. Subsequently, he conducted research in the magnetostrictive properties of soft-ferromagnetic materials at microwave frequencies with the Optics Division of NRL. In 1994 he joined SFA, Inc. engaged in materials research for antenna applications. In 1998 he joined NRL as a research physicist responsible for the development of the NRL Ultra-Near Field Laboratory and associated measurement and analytical techniques used to characterize the electromagnetic scattering from complex targets.

L. N. Medgyesi-Mitschang received the B.S. (1961), M.S. (1962) and D.Sc. (1967) degrees in Electrical Engineering from Washington University, St. Louis. In 1967 he joined the McDonnell Douglas Corporation (MDC) as a research scientist in the corporate laboratory where he developed new microwave, radiometric, and interferometric diagnostic techniques for high temperature plasmas. Subsequently, during the past two decades he pioneered new techniques in computational electromagnetics for scattering from complex targets, analysis of airborne arrays, and simulation of wave phenomena in composite materials. He has been a principal investigator on numerous R&D programs for the US Tri-Services and national labs. He has served on special assignments for the MDC Corporate Office on technology integration, assessment and strategic planning. In 1991 he was elected a Senior Technical Fellow of MDC. With the merger of MDC with the Boeing Company, he was named

Staff Director of the Computational Electromagnetics Group within Phantom Works, the Boeing advanced R&D organization. In 1999, he assumed the responsibilities of a Chief Scientist at the Naval Research Laboratory. Dr. Medgyesi-Mitschang has authored numerous papers and chapter length contributions in the field of electromagnetics, antennas, numerical analysis and computer simulation/modeling. He is a co-editor of *Computational Electromagnetics*, IEEE Press. He served as Guest Editor of *IEEE Proceedings*, was Associate Editor of *IEEE Transactions on Antennas and Propagation* and ADCOM member of the *IEEE MTT-S*. He is a Fellow of the IEEE, Associate Fellow of the AIAA, member of URSI (Commission B), ACES, Tau Beta Pi, Eta Kappa Nu and Sigma Xi.

D. W. Forester received his B.S. in Physics from Berea College, Kentucky in 1959. He received his M.S. (1961) and Ph.D. (1964) degrees in Physics from the University of Tennessee. He was Assistant Professor of Physics at the University of Nebraska (1964–66) and the Georgia Institute of Technology (1966–69). In 1969 he joined the Magnetism Branch of the Naval Research Laboratory (NRL). Since then he has performed and managed research in areas of magnetic materials, hydrogen storage, antenna isolation, electromagnetic-acoustic similarity, photonic bandgap and "left-handed" materials. He currently serves as Head of the Signature Technology Office in the Systems Directorate of NRL.